Information Transduction Capacity of Mitochondrial Retrograde Signaling

Shao-Ting Chiu[1] **and An-Chi Wei**[1]

[1]Department of Electrical Engineering, National Taiwan University, Taipei, Taiwan
*b03901045@ntu.edu.tw; acwei86@ntu.edu.tw

ABSTRACT

Mitochondrion is the powerhourse of eukaryotic cells, which participates in crucial cellular processes such as ATP production and intermediate metabolism. Though mitochondria possess their own genomes, most of the mitochondrial proteins are encoded in nucleus. Therefore, the retrograde response between mitochondria and nucleus is essential for the mitochondrial quality control which includes removing damaged mitochondria and fission-fusion dynamics. However, all the mitochondria use the same biological pathway to interact with nucleus genome, and it is still unclear that how this multiplexing problem reduces the information transduction capacity of mitochondrial retrograde signaling. In this project, the agent-based model is used to simulate the information transmission rate under the influences of mitochondrial dynamics.

Keywords: mitochondrial dynamics, retrograde signalling, information theory

Introduction

Mitochobndrial defects have been associated with many human diseases, espeically in the diseases related to neuron degeneration or aging[1–4]. Therefore, mitochondiral quality control is essential to maintain cell viability. Although mitochondria are semi-autonomous organelles in cytosol, which means they have their own genome and other metabolic systems which make them more independent than other organelles, most of mitochondiral genes are still encoded in nucleus genome. Therefore, the communication between mitochondria and nucleus, also known as retrograde response, is essential for maintaining mitochondrial function and genome stability[5,6]. It is interesting to note that when mitochondria are damaged, their statuses will report to nucleus by sending molecular singals or interfering with metabolic system, and then enabling a cell to coordinate mitochondrial biogenesis. Therefore, mitochondrial quality control depends on the feedback of mitochondrial network status, which is known as mitochondrial retrograde signalling.

The most detailed mitochondrial retrograde signaling is RTG pathway discovered in budding yeast[7]. There are three positive regulatory factors including Rtg1/2/3 (Table 1), and other four negative regulatory factors participating in RTG pathway[8]. In budding yeast, Rtg2 is mitochondrial sensor which is activated while mitochondria are dysfunctional. The activated Rtg2 results in dephosphorlation of Rtg3 by inhibiting Mks1-Bmh protein complex. Furthermore, dephosphorylated Rtg3 binds with Rtg1 and forms transcriptional factor which regulates mitochondiral retrograde response by traslocating into nucleus[9,10]. However, it is still unclear how a cell detects a particular mitochondiral dysfunction, while the known examples are adenosine triphosphate (ATP), reactive oxygen species (ROS), and mitochondrial membrane potential ($\Delta\psi_m$) to name a few.

Furthermore, a cell usually processes a number of mitochondria, while each of them shares same retrograde signaling pathway (RTG pathway), resulting in a multiplexing problem which was first described

in telecommunications. Sharing channel may lead to unwanted cross-talk. multiple analog signals can be combined into one signal via a shared medium.

Biological noise restricts the ability of cell to gather information from input. In eukaryotic cells like budding yeast, in which mitochondira interact with one cell nucleus via the same biochemical channel. It is still unclear how biological system manages multiplexing communication network in mitochondrial retrograde response.

Methods

The equations were solved by Sympy (http://www.sympy.org) and Scipy (https://www.scipy.org), which are Python-based toolboxes for symbolic mathematics. Source codes are shown in supplemental materials.

Results

Biochemical Network components of RTG Pathway

In order to investigate information transmission properties, it is better to describe mathematical equations of mitochondrial retrograde signalling with proper notations and assumptions. The following sections describe the differential equation-based framework of yeast RTG pathway (Figure 2).

1. Input vector: There are multiple inputs of retrograde signalling, the vector form is described in equation 1 and Figure 1.

$$\vec{MT} := MT_1, ..., MT_N \tag{1}$$

where N is the total number of mitochondria.

2. Input coding: Though mitochondrial dysfunction activates Rtg2 to indirectly promote the dephosphorylation of Rtg3[9,10], it is still unclear how Rtg2 senses mitochondrial dysfunction. Therefore, I separated the sensing mechanism into two parts: hypothetical Signal (S, equation 2) and Hill relation[11] between activated Rtg2 and hypothetical signal. Assume the hypothetical signal (S) is the linear combination of mitochondrial volume and damaged state (equation 3, 4, 5)

$$S = \sum_{i=1}^{N} Volume_{MT_i} \times Damaged_{MT_i} \tag{2}$$

The damaged value (eauation 5) can be defined as drop of mitochondrial membrane potential ($\Delta\psi_m$)[12] or reduced ATP production rate[13] which can activate Rtg2 protein and induce retrograde signalling. The distributions of $Volume_{MT_i}$ and $Damaged_{MT_i}$ can be estimated from the mitochondrial Netlogo model[12] which provides simulation environmenet of mitochondrial fission-fussion dynamics and reasonable biological parameters.

$$Volume_{MT_i} \subset [V_{min}, V_{max}] \tag{3}$$

$$V_{max} = \frac{4}{3} h \times Area_{MT_i} \tag{4}$$

In mitochondrial Netlogo model[12], mitochondrial volume is measured in area (μm^2), the mitochondrial volume is re-scaled from area in equation 4 with mitochondrial height (h). Besides, the reasonable value of mitochondrial height for yeast needs to fulfill the condition $Volume_{MT_i} \subset [0.3,4]\mu m^2$[14].

$$Damaged_{MT_i} := \{0,1\} \tag{5}$$

where 0 represents healthy state, and 1 represents damaged state of mitochondrion i (MT_i)

3. Channel ν with M species: Mitochondrial retrograde signalling is modelled as communication channel ν which includes retrograde signal proteins (Table 1) and their subsequent heterodimers. The vector form of channel ν is written in equation 6.

$$V_1, ..., V_M \tag{6}$$

where M is the total number of proteins involved in network.

The index of each component is defined below:

$$\begin{aligned}
V_1 &:= Rtg2_C^{ina} \\
V_2 &:= Rtg2_C^{act} \\
V_3 &:= Rtg3_C^{P} \\
V_4 &:= Rtg3_C^{U} \\
V_5 &:= Rtg3_N^{P} \\
V_6 &:= Rtg3_N^{U} \\
V_7 &:= Rtg1_C \\
V_8 &:= Rtg1_N \\
V_9 &:= Rtg1 - 3_C^{P} \\
V_{10} &:= Rtg1 - 3_C^{U} \\
V_{11} &:= Rtg1 - 3_N^{P} \\
V_{12} &:= Rtg1 - 3_N^{U} \\
V_{13} &:= Bmh_C \\
V_{14} &:= Bmh - Mks1_C \\
V_{15} &:= Mks1 - Rtg2_C^{ina} \\
V_{16} &:= Mks1 - Rtg2_C^{act} \\
V_{17} &:= Mks1_C
\end{aligned} \tag{7}$$

where the modificaton (M) and location (L) states are labeled in the form: $Protein_L^M$. Here are the notations:

$$\begin{aligned}
Location &:= \{Nucleus(N), Cytoplasm(C)\} \\
Modification &:= \{Phopholated(P), Partiallydephosphated(U), activated(act), inactivated(ina)\}
\end{aligned} \tag{8}$$

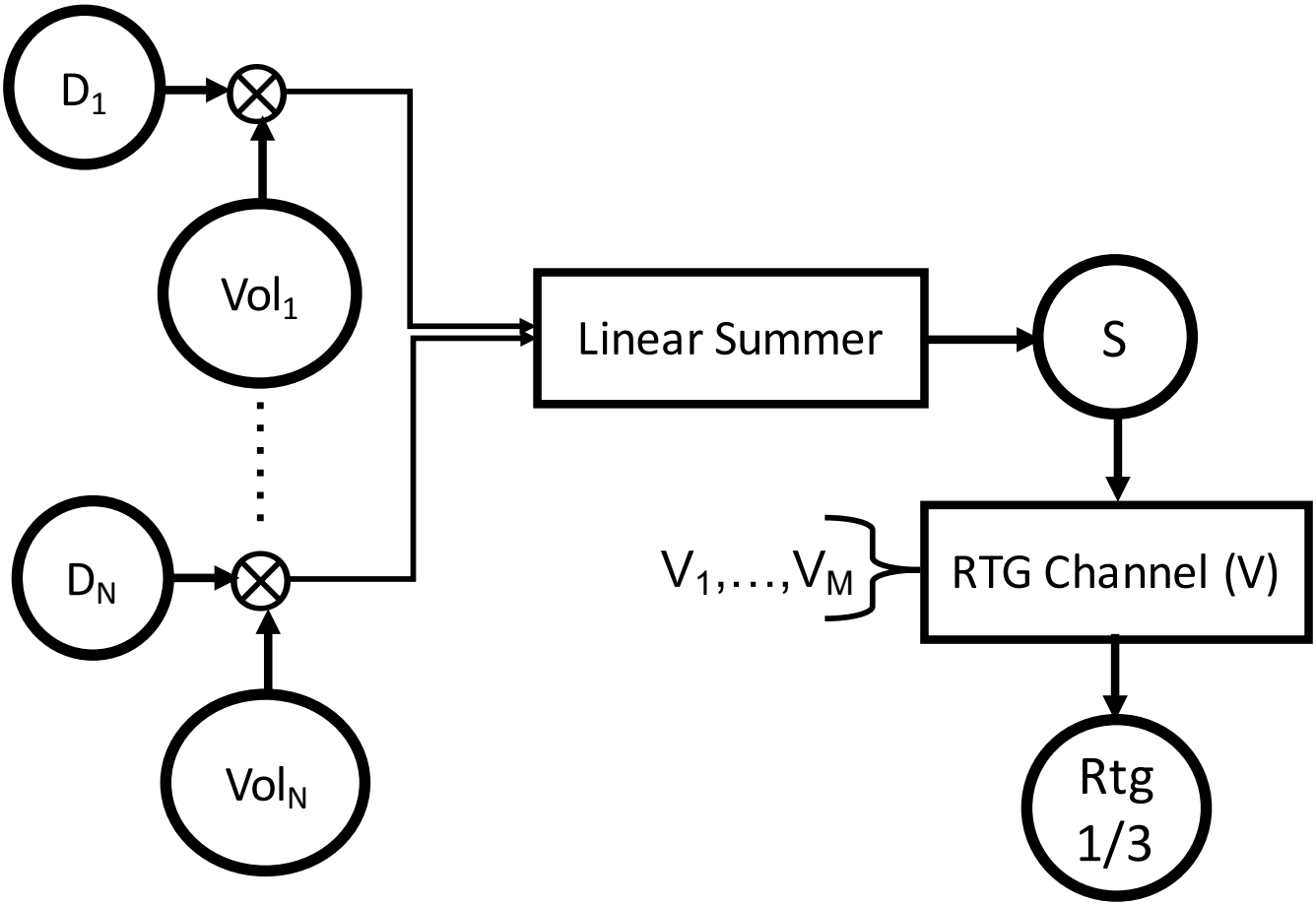

Figure 1. Diagram of mitochondrial retrograde signalling

Table of RTG-associated Proteins[9,10,13]		
Protein	Function	Human homolog
Rtg1-Rtg3	Activates retrograde response	MYC-MAX
Rtg2	Promotes translocation of Rtg1-Rtg3 from cytosol to nucleus; binds with Mks1	unclear[9]
Mks1	Phospholates Rtg3; downregulates RTG pathway	MKS1
Bmh1 or Bmh2	Binds with Mks1, and forms Bmh1/2-Mks1 to phosphate Rtg3	YWHAE

Table 1. RTG-associated proteins. This table contains proteins which are associated with yeast mitochondrial retrograde respone, and human homologs are also referenced.

Reactions of RTG Pathway

The notations are described in equation 8.

1. RTG2 and S: Input layer

$$Rtg2_C^{ina} \rightarrow^{hill_{act}(S,k_1,ka_1,n_1)} Rtg2_C^{act} \tag{9}$$

$$Rtg2_C^{act} \rightarrow^{k2} Rtg2_C^{ina} \tag{10}$$

2. RTG2, BMH AND MKS1: Switch layer

$$Mks1_C + Rtg2_C^{ina} \rightleftharpoons_{kn3}^{k3} Mks1 - Rtg2_C^{ina} \tag{11}$$

$$Mks1_C + Rtg2_C^{act} \rightleftharpoons_{kn4}^{k4} Mks1 - Rtg2_C^{act} \tag{12}$$

$$Mks1_C + Bmh_C \rightleftharpoons_{kn5}^{k5} Mks1 - Bmh_C \tag{13}$$

3. RTG3: Phosphorylation (P) and partially dephosphorylation (U)

$$Rtg3_C^U \rightarrow^{hill_{act}([Mks1-Bmh_C],k_6,ka_6,n_6)} Rtg3_C^P \tag{14}$$

$$Rtg3_C^P \rightarrow^{k7} Rtg3_C^U \tag{15}$$

$$Rtg3_N^P \rightleftharpoons_{kn8}^{k8} Rtg3_N^U \tag{16}$$

4. RTG3: Translocation

$$Rtg3_C^U \rightleftharpoons_{kn9}^{k9} Rtg3_N^U \tag{17}$$

$$Rtg3_C^P \rightleftharpoons_{kn10}^{k10} Rtg3_N^P \tag{18}$$

5. RTG1 and RTG3

$$Rtg3_C^U + Rtg1_C \rightleftharpoons_{kn11}^{k11} Rtg1/3_C^U \tag{19}$$

$$Rtg3_C^P + Rtg1_C \rightleftharpoons_{kn12}^{k12} Rtg1/3_C^P \tag{20}$$

$$Rtg3_N^U + Rtg1_N \rightleftharpoons_{kn13}^{k13} Rtg1/3_N^U \tag{21}$$

$$Rtg3_N^P + Rtg1_N \rightleftharpoons_{kn14}^{k14} Rtg1/3_N^P \tag{22}$$

6. RTG1/3: Output layer

$$Rtg1/3^U_C \rightleftharpoons^{k_{15}}_{kn_{15}} Rtg1/3^U_N \tag{23}$$

$$Rtg1/3^P_C \rightleftharpoons^{k_{16}}_{kn_{16}} Rtg1/3^P_N \tag{24}$$

Differential Equation-based Framework

By applying mass action kinetics and hill functions to retrograde proteins (RTG proteins), the mitochondrial retrograde signalling are described from equation 25 to equation 41 based on notations described in equation 7, 6, 8.

$$\frac{d}{dt}V_1 := \frac{d}{dt}[Rtg2^{ina}_C] = -k_1\frac{S^{n_1}}{ka_1+S^{n_1}} + k_2[Rtg2^{act}_C] - k_3[Rtg2^{ina}_C][Mks1_C] + kn_3[Rtg2^{ina} - Mks1_C] \tag{25}$$

$$\frac{d}{dt}V_2 := \frac{d}{dt}[Rtg2^{act}_C] = k_1\frac{S^{n_1}}{ka_1+S^{n_1}} - k_2[Rtg2^{act}_C] - k_4[Rtg2^{act}_C][Mks1_C] + kn_4[Rtg^{act}_2 - Mks1_C] \tag{26}$$

$$\begin{aligned}\frac{d}{dt}V_3 &:= \frac{d}{dt}[Rtg3^P_C] \\ &= k_6\frac{[Bmh-Mks1_C]^{n_6}}{ka_6+[Bmh-Mks1_C]^{n_6}} - \\ &k_7[Rtg3^P_C] - k_{10}[Rtg3^P_C] + kn_{10}[Rtg3^P_N] - \\ &k_{12}[Rtg3^P_C][Rtg1_C] + kn_{12}[Rtg1/3^P_C]\end{aligned} \tag{27}$$

$$\begin{aligned}\frac{d}{dt}V_4 &:= \frac{d}{dt}[Rtg3^U_C] \\ &= -k_6\frac{[Bmh-Mks1_C]^{n_6}}{ka_6+[Bmh-Mks1_C]^{n_6}} \\ &+ k_7[Rtg3^P_C] - k_9[Rtg3^U_C] + kn_9[Rtg3^U_N] \\ &- k_{11}[Rtg3^U_C][Rtg1_C] + kn_{11}[Rtg1/3^U_C]\end{aligned} \tag{28}$$

$$\begin{aligned}\frac{d}{dt}V_5 &:= \frac{d}{dt}[Rtg3^P_N] = -k_8[Rtg3^P_N] + \\ &kn_8[Rtg3^U_N] + k_{10}[Rtg3^P_C] - kn_{10}[Rtg3^P_N] - \\ &k_{14}[Rtg^P_N][Rtg1_N] + kn_{14}[Rtg1/3^P_N]\end{aligned} \tag{29}$$

$$\begin{aligned}\frac{d}{dt}V_6 &:= \frac{d}{dt}[Rtg3^U_N] = k_8[Rtg3^P_N] - \\ &kn_8[Rtg3^U_N] + k_9[Rtg3^U_C] - kn_9[Rtg3^U_N] - \\ &k_{13}[Rtg^U_N][Rtg1_N] + kn_{13}[Rtg1/3^U_N]\end{aligned} \tag{30}$$

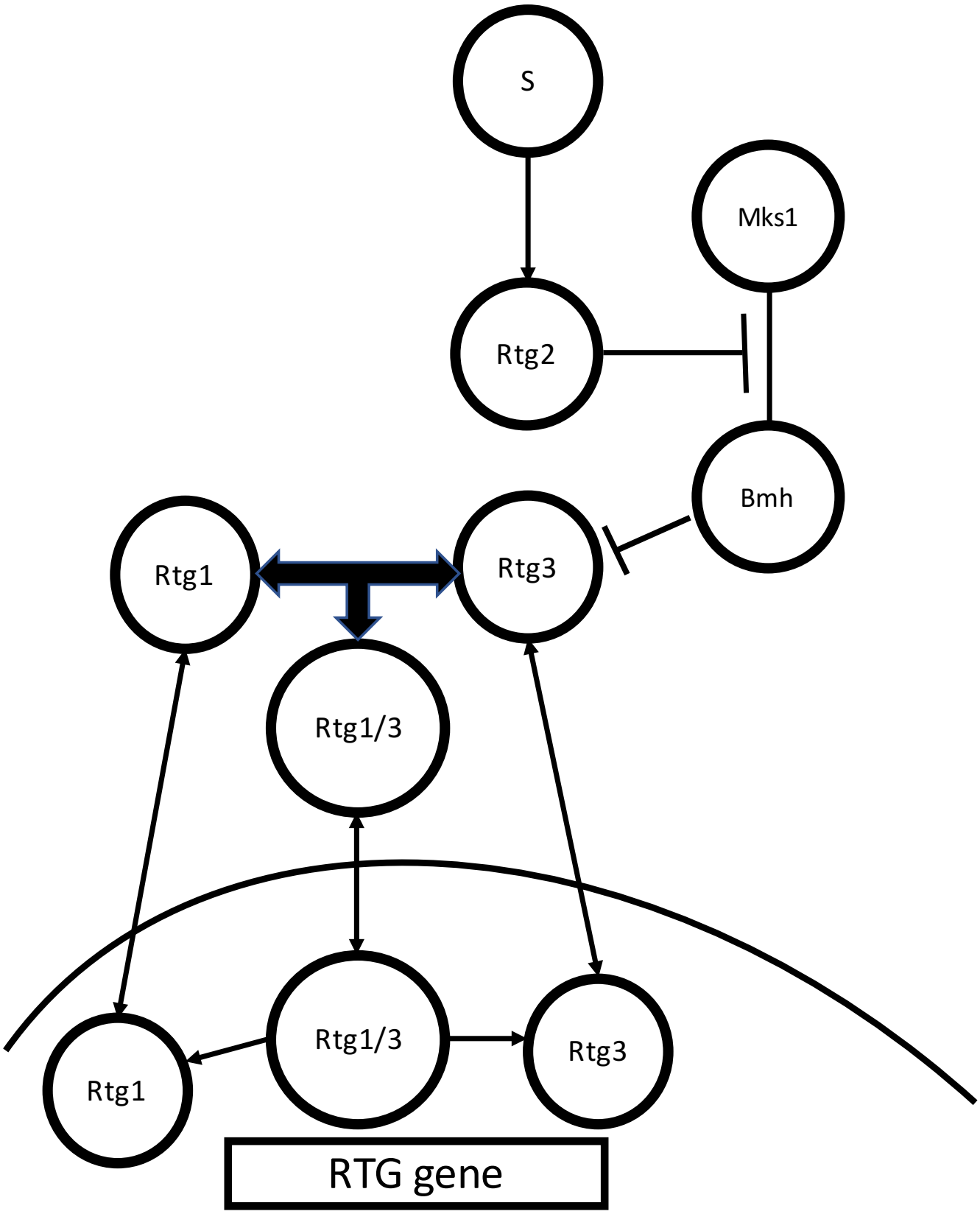

Figure 2. Diagram of differential equation-based model

$$\begin{aligned}\frac{d}{dt}V_7 := \frac{d}{dt}[Rtg1_C] &= -k_{11}[Rtg3^U_C][Rtg1_C] \\ &+ kn_{11}[Rtg1/3^U_C] - k_{12}[Rtg3^P_C][Rtg1_C] \\ &+ kn_{12}[Rtg1/3^P_C] - k_{17}[Rtg1_C] + k_{17}[Rtg1_N]\end{aligned} \tag{31}$$

$$\begin{aligned}\frac{d}{dt}V_7 := \frac{d}{dt}[Rtg1_C] &= -k_{11}[Rtg3^U_C][Rtg1_C] \\ &+ kn_{11}[Rtg1/3^U_C] - k_{12}[Rtg3^P_C][Rtg1_C] \\ &+ kn_{12}[Rtg1/3^P_C] - k_{17}[Rtg1_C] + k_{17}[Rtg1_N]\end{aligned} \tag{32}$$

$$\begin{aligned}\frac{d}{dt}V_8 := \frac{d}{dt}[Rtg1_N] &= -k_{13}[Rtg3^U_N][Rtg1_N] \\ &+ kn_{13}[Rtg1/3^U_N] - k_{14}[Rtg3^P_N][Rtg1_N] \\ &+ kn_{14}[Rtg1/3^P_N] + k_{17}[Rtg1_C] - k_{17}[Rtg1_N]\end{aligned} \tag{33}$$

$$\frac{d}{dt}V_9 := \frac{d}{dt}[Rtg1/3^P_C] = k_{12}[Rtg3^P_C][Rtg1_C] - kn_{12}[Rtg1/3^P_C] - k_{16}[Rtg1/3^P_C] + kn_{16}Rtg1/3^P_N \tag{34}$$

$$\frac{d}{dt}V_{10} := \frac{d}{dt}[Rtg1/3^U_C] = k_{11}[Rtg3^U_C][Rtg1_C] - kn_{11}[Rtg1/3^U_C] - k_{15}[Rtg1/3^U_C] + kn_{15}[Rtg1/3^U_N] \tag{35}$$

$$\frac{d}{dt}V_{11} := \frac{d}{dt}[Rtg1/3^P_N] = k_{14}[Rtg3^P_N][Rtg1_N] - kn_{14}[Rtg1/3^P_N] + k_{16}[Rtg1/3^P_C] - kn_{16}[Rtg1/3^P_N] \tag{36}$$

$$\frac{d}{dt}V_{12} := \frac{d}{dt}[Rtg1/3^U_N] = k_{13}[Rtg3^U_N][Rtg1_N] - kn_{13}[Rtg1/3^U_N] + k_{15}[Rtg1/3^U_C] - kn_{15}[Rtg1/3^U_N] \tag{37}$$

$$\frac{d}{dt}V_{13} := \frac{d}{dt}[Bmh_C] = -k_5[Mks1_C][Bmh_C] + kn_5[Mks1 - Bmh_C] \tag{38}$$

$$\frac{d}{dt}V_{14} := \frac{d}{dt}[Mks1 - Bmh_C] = k_5[Mks1_C][Bmh_C] - kn_5[Mks1 - Bmh_C] \tag{39}$$

$$\frac{d}{dt}V_{15} := \frac{d}{dt}[Mks1 - Rtg2^{ina}_C] = k_3[Mks1_C][Rtg2^{ina}_C] - kn_3[Mks1 - Rtg2^{ina}_C] \tag{40}$$

$$\frac{d}{dt}V_{16} := \frac{d}{dt}[Mks1 - Rtg2^{act}_C] = k_4[Mks1_C][Rtg2^{act}_C] - kn_4[Mks1 - Rtg2^{act}_C] \tag{41}$$

Necessary requirements

In order to define parameter space of equation 9-24, the differential equation-based framwork should coincide on the experiment results. Fortunately, the biological functionality has been investigated by a group of deletions of RTG pathway[10] with GFP-labelled proteins. Sekito et al.[10] describes 14 localizaton patterns by deletions of Rtg1, Rtg2, and Rtg3. Their results are summarized in Figure 5, and the derived mathematical model has to fullfill those phenomenon identified in yeast.

Yeast mitochondrial 3D structure can be measured by Delta Vision microscopy with GFP labeling (Figure 3, 4).

The Boolean algebra is used to describe those phenomenon.

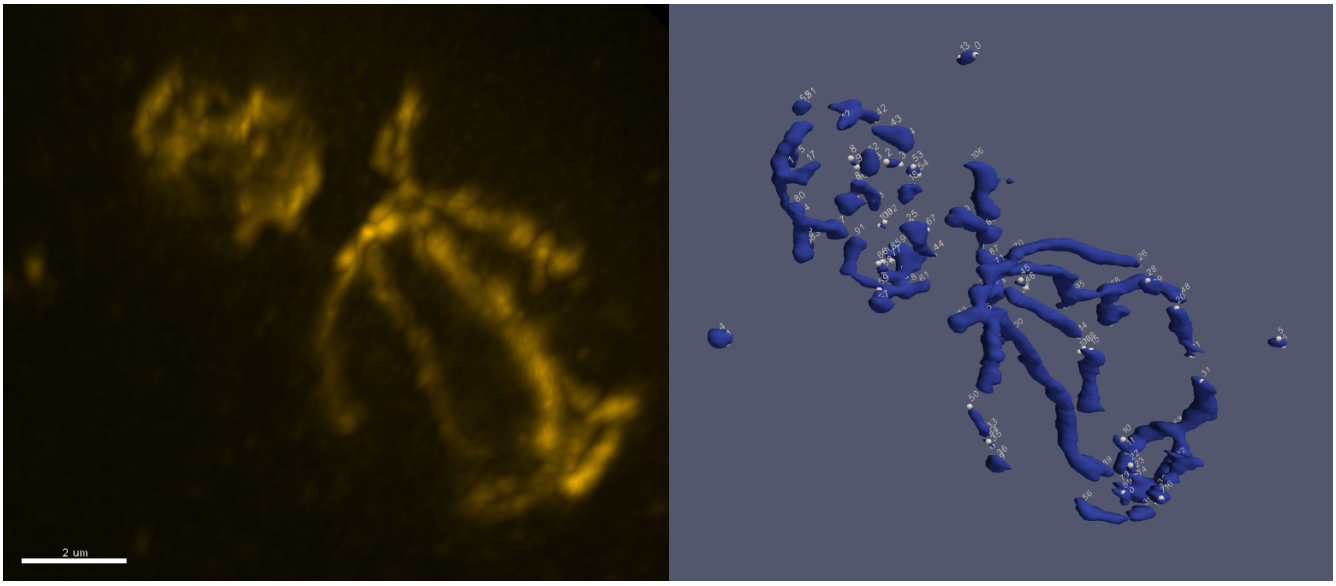

Figure 3. Mitochondrial network. (a) 3D mitochondrial structure labeled with MitoTracker Red (b) Mitochondrial network

Property	$[*-Rtg1_*]$	$[Rtg2_C]$	**S**
$[*-Rtg3^*_C] > [*-Rtg3^*_N]$	>0	>0	$=0$
$[*-Rtg3^*_C] > [*-Rtg3^*_N]$	>0	$=0$	$=0$
$[*-Rtg3^*_C] > [*-Rtg3^*_N]$	>0	=0	=high
$[*-Rtg3^*_C] < [*-Rtg3^*_N]$	>0	>0	=high
$[*-Rtg3^*_C] < [*-Rtg3^*_N]$	=0	>0	=0
$[*-Rtg3^*_C] < [*-Rtg3^*_N]$	=0	>0	=high
$[*-Rtg3^*_C] < [*-Rtg3^*_N]$	=0	=0	=0
$[*-Rtg3^*_C] < [*-Rtg3^*_N]$	=0	=0	=high

Table 2. Properties of Rtg3p-GFP localization.

1. Properties of Rtg3 Translocation (Table 2)

   where

$$\begin{aligned}[*-Rtg3^*_C] &:= [Rtg1-Rtg3^P_C]+[Rtg1-Rtg3^U_C]+[Rtg3^U_C]+[Rtg3^P_C]\\ [*-Rtg3^*_N] &:= [Rtg1-Rtg3^P_N]+[Rtg1-Rtg3^U_N]+[Rtg3^U_N]+[Rtg3^P_N]\end{aligned} \quad eq: rtg-summation-chemical2 \tag{42}$$

$$\begin{aligned}[*-Rtg1_*] :=& [Rtg1_C]+[Rtg1_N]+[Rtg1-Rtg3^P_C]\\ &+[Rtg1-Rtg3^U_C]+[Rtg1-Rtg3^P_N]+[Rtg1-Rtg3^U_N]\end{aligned} \tag{43}$$

2. Properties of Rtg1 Translocation (Table 3)

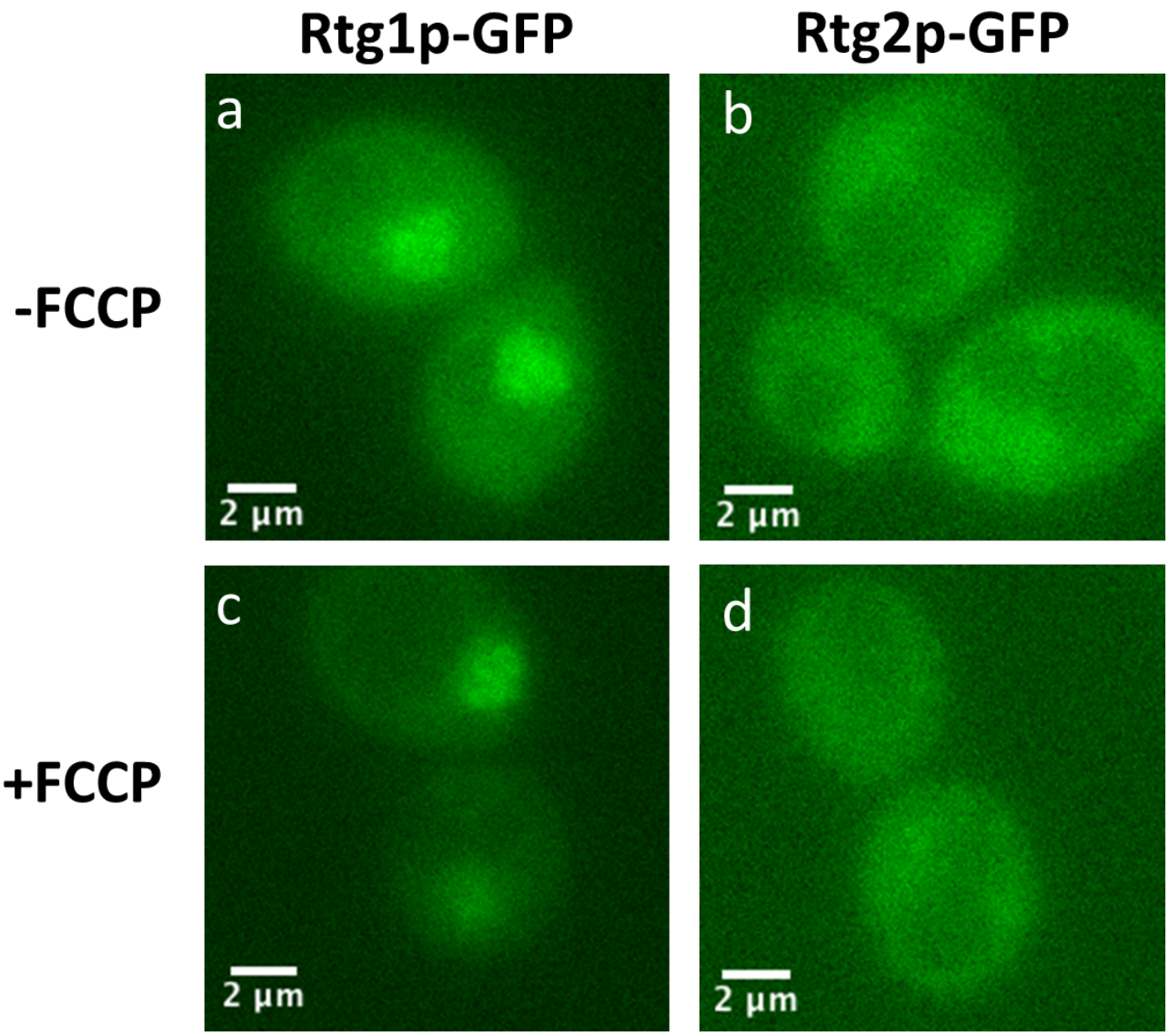

Figure 4. (a)(c) Subcellular localization Rtg1p which transfers to nucleus in FCCP treatment. (b)(d) Subcellular localization of Rtg2p which is insensitive to FCCP treatment (-FCCP: 0 μM FCCP; +FCCP: 15 μM FCCP)

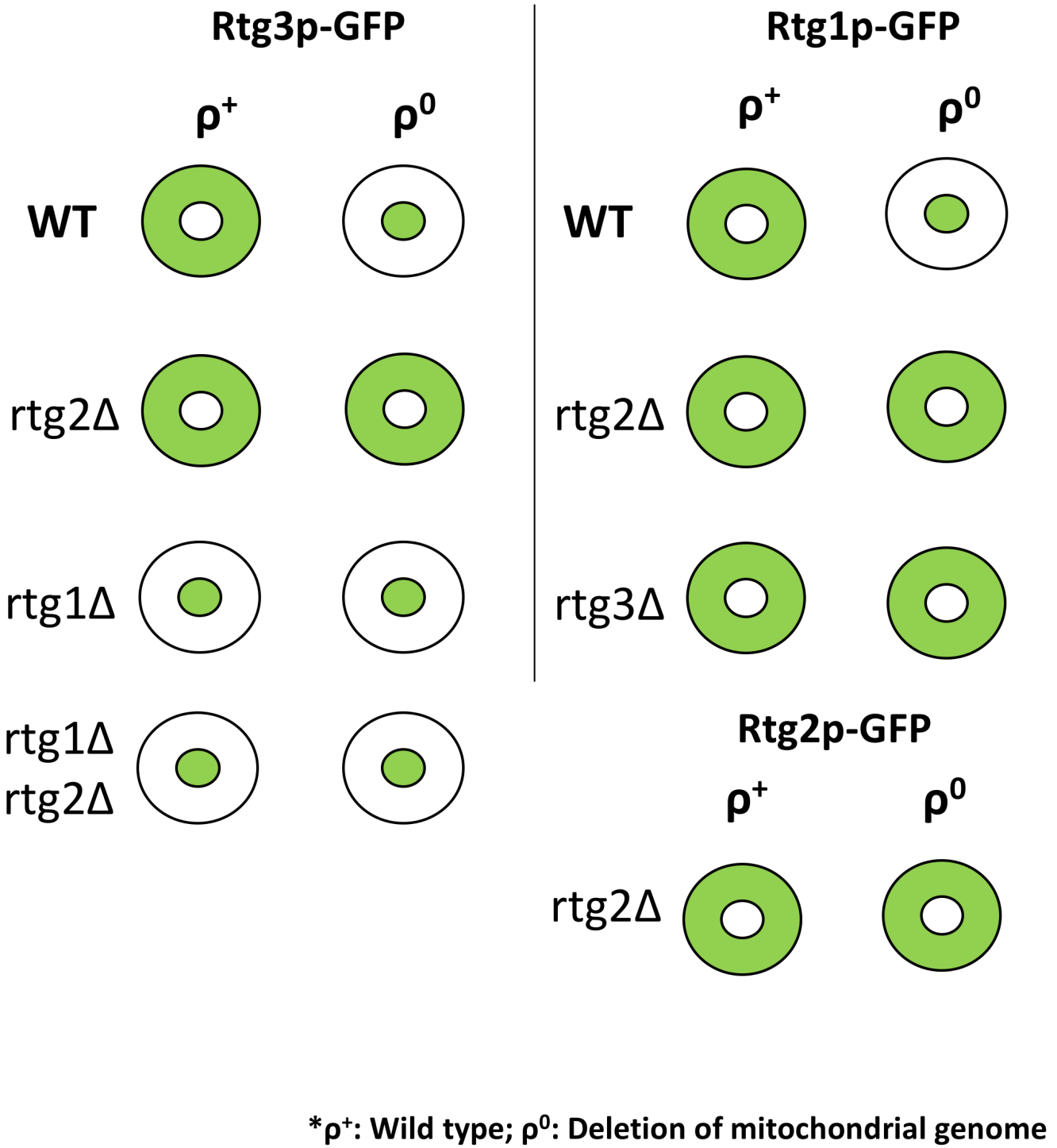

Figure 5. Properties of translocation of RTG proteins. Outer circle represents cell membrane,and inner circle represents nuclear membrane. The location of GFP-labelled protein of deletion strins are graphically displayed.

$[*-Rtg1_C] > [*-Rtg1_N]$	>0	>0	=0
$[*-Rtg1_C] > [*-Rtg1_N]$	>0	=0	=0
$[*-Rtg1_C] > [*-Rtg1_N]$	>0	=0	=high
$[*-Rtg1_C] > [*-Rtg1_N]$	=0	>0	=0
$[*-Rtg1_C] > [*-Rtg1_N]$	=0	>0	=high
$[*-Rtg1_C] < [*-Rtg1_N]$	>0	>0	=high

Table 3. Properties of Rtg3p-GFP localization. Deleted protein are set to 0, and wild type protein are assumed to be greater than 0. The notation defined in equation 44.

where

$$\begin{aligned}[*-Rtg1_C] &:= [Rtg1_C] + [Rtg1 - Rtg3^P_C] + [Rtg1 - Rtg3^U_C] \\ [*-Rtg1_N] &:= [Rtg1_N] + [Rtg1 - Rtg3^P_N] + [Rtg1 - Rtg3^U_N] \\ [Rtg3^*_\#] &:= [*-Rtg3^*_C] + [*-Rtg3^*_N]\end{aligned} \tag{44}$$

Truth Table and Karnaugh Map

Seiko et al. describes the properties of retrograde pathway by measuring deletion with GFP-labelled protein, which is binary manipulation, to say, the test protein can be wild type or deleted. Therefore, I applied Boolean function to summarize the result, and use Karnaugh map to simplify the relation between channel factors and output. In this part, output is defined as the translocation of trancription factors (equation 45, 47). The requirements in Table 2, 3 are trasformed into Boolean algebra and simplied by Karnaugh map.

Condition	Mapping to Boolean Space
$[*-Rtg3^*_C] < [*-Rtg3^*_N]$	1
$[*-Rtg3^*_C] > [*-Rtg3^*_N]$	0
$[*-Rtg1_*] > 0$	1
$[*-Rtg1_*] = 0$	0
$[Rtg2_C] > 0$	1
$[Rtg2_C] = 0$	0
$S = high$	1
$S = 0$	0

Table 4. Definition of boolean algebra on translocation of Rtg3

$$Translocation_{Rtg3} := \begin{cases} 1 \text{ if } [*-Rtg3^*_C] < [*-Rtg3^*_N] \\ 0 \text{ if } [*-Rtg3^*_C] > [*-Rtg3^*_N] \end{cases} \tag{45}$$

Result:

$$Translocation_{Rtg3} = \sim Bool([*-Rtg1_*]) + Bool([Rtg2_C]) \times S \tag{46}$$

This model expects (0,0,0,1)

$Bool([*-Rtg1_*])$	$Bool([Rtg2_C])$	S	$Translocation_{Rtg3}$ (Output)
0	0	0	x
0	0	1	1
0	1	0	1
0	1	1	1
1	0	0	0
1	0	1	0
1	1	0	0
1	1	1	1

Table 5. Truth table of Rtg3 translocation properties, where x is "don't care term", for some relations haven't verified in paper[10].

Condition	Mapping to Boolean Space
$[*-Rtg1_C] > [*-Rtg1_N]$	0
$[*-Rtg1_C] < [*-Rtg1_N]$	1
$[Rtg3^*_\#] > 0$	1
$[Rtg3^*_\#] = 0$	0
$[Rtg2_C] > 0$	1
$[Rtg2_C] = 0$	0
$S = high$	1
$S = 0$	0

Table 6. Definition of boolean algebra on translocation of Rtg3

Rtg1p Translocation

Definition

$$Translocation_{Rtg1} := \begin{cases} 1 \text{ if } [*-Rtg1_C] < [*-Rtg1_N] \\ 0 \text{ if } [*-Rtg1_C] > [*-Rtg1_N] \end{cases} \tag{47}$$

$$Transduction_{Rtg1} = Bool([Rtg3^*_\#]) \times Bool([Rtg2_C]) \times S \tag{48}$$

This model expects (0,0,0,0), (0,0,1,0)

Important Concepts in Information Theory

The information theory is usually apply to electronic communication system, and mitochondrial retrograde response could be analog to information passage.

1. Shannon's information

$$H(S) = -\sum_{s \in s} P(s) log P(s) \tag{49}$$

where S is a random variable

2. Mutual information

$Bool([Rtg3^*_{\#}])$	$Bool([Rtg2_C])$	S	$Translocation_{Rtg1}$ (Output)
0	0	0	x
0	0	1	x
0	1	0	0
0	1	1	0
1	0	0	0
1	0	1	0
1	1	0	0
1	1	1	1

Table 7. Truth table of Rtg1 translocation properties, where x is "don't care term", for some relations haven't verified in paper. The concentration of deleted protein is 0, otherwise 1, and the translocation is 1 when the concentration of the protein in nucleus is higher than in cytosol[10].

(a) Mutual information is symmetric.

$$\begin{aligned} I(S;R) &= H(S) - H(S|R) \\ &= H(R) - H(R|S) \\ &= I(R;S) \end{aligned} \tag{50}$$

(b) $I(S;R)$ is a concave function of P_S for fixed $P_{R|S}$

3. Channel capacity

(a) For a discrete memoryless channel $(S, P_{R|S}, R)$, the maximum rate of information transmission with vanishing error probability is

$$C = max_{P_S(.)} I(S;R), \tag{51}$$

also known as channel capacity[15].

Frequency Response

We can rewrite equation 9 to 24 into state-space formula, and calculate frequency response of the retrograde signalling. The content of matrices are included in supplemental materials.

$$\frac{d}{dt}\mathbf{x} = f(\mathbf{x}(t), \mathbf{u}(t)) = \mathbf{A}x(t) + \mathbf{B}u(t) \tag{52}$$

$$y(t) = h(\mathbf{x}(t), \mathbf{u}(t)) = \mathbf{C}x(t) + \mathbf{D}u(t) \tag{53}$$

Discussion

In this project, the mathematical model of mitochondrial retrograde signalling is constucted by differential equation-based framework. The frequency response may be derived from state-space formula52,53. While the explicit solution may require parallel computation strategies.

This study may lead to a better understanding of mitochondrial retrograde signalling. In so doing it seeks to contribute to our growing understanding of how and to what extent interaction between mitochondria and nucleus.

Conclusion

Differential equation-based framework of mitochondrial retrograde signalling in yeast is constructed based on protein-protein interaction and deletion experiments in published papers[10,16]. Besides, Boolean logic functions are applied and simplified to describe the binary relation between Rtg1/2/3 proteins.

The system described here could serve as the basis for a study of information-transmission theory of mitochondrial-to-nucleus communication.

References

1. Cwerman-Thibault, H., Sahel, J.-A. & Corral-Debrinski, M. Mitochondrial medicine: to a new era of gene therapy for mitochondrial DNA mutations. *J. inherited metabolic disease* **34**, 327–344 (2011).
2. Wallace, D. C. Mitochondrial function and cancer. *Nat. Rev. Cancer* **12**, 1 (2012).
3. Bonawitz, N. D., Rodeheffer, M. S. & Shadel, G. S. Defective Mitochondrial Gene Expression Results in Reactive Oxygen Species-Mediated Inhibition of Respiration and Reduction of Yeast Life Span. *Mol. Cell. Biol.* **26**, 4818–4829 (2006).
4. Jafri, M. S. & Kumar, R. *Modeling mitochondrial function and its role in disease*, vol. 123 (Elsevier Inc., 2014), 1 edn.
5. Jazwinski, S. M. The retrograde response: When mitochondrial quality control is not enough. *Biochimica et Biophys. Acta - Mol. Cell Res.* (2013).
6. Kaniak-Golik, A. & Skoneczna, A. Mitochondria-nucleus network for genome stability. *Free. Radic. Biol. Medicine* **82**, 73–104 (2015).
7. Liao, X. S., Small, W. C., Srere, P. A. & Butow, R. A. Intramitochondrial functions regulate nonmitochondrial citrate synthase (CIT2) expression in Saccharomyces cerevisiae. *Mol. cellular biology* **11**, 38–46 (1991).
8. Dilova, I., Chen, C. Y. & Powers, T. Mks1 in concert with TOR signaling negatively regulates RTG target gene expression in S. cerevisiae. *Curr. Biol.* **12**, 389–395 (2002).
9. Jazwinski, S. M. & Kriete, A. The yeast retrograde response as a model of intracellular signaling of mitochondrial dysfunction. *Front. Physiol.* **3 MAY**, 1–12 (2012).
10. Sekito, T., Thornton, J. & Butow, R. A. Mitochondria-to-nuclear signaling is regulated by the subcellular localization of the transcription factors Rtg1p and Rtg3p. *Mol. biology cell* **11**, 2103–15 (2000).
11. Ingalls, B. P. *Mathematical Modelling in Systems Biology : An Introduction*, vol. 53 (2014). arXiv:1011.1669v3.
12. Dalmasso, G. *et al.* Agent-Based Modeling of Mitochondria Links Sub-Cellular Dynamics to Cellular Homeostasis and Heterogeneity. *PLOS ONE* **12**, e0168198 (2017).
13. Rios-Anjos, R. M., de Lima Camandona, V., Bleicher, L. & Ferreira-Junior, J. R. Structural and functional mapping of rtg2p determinants involved in retrograde signaling and aging of saccharomyces cerevisiae. *PloS one* **12**, e0177090 (2017).
14. Rafelski, S. M. *et al.* Mitochondrial Network Size Scaling in Budding Yeast. *Sci.* **338**, 822–824 (2012).
15. Thomas M. Cover & Thomas, J. A. *Elements of Information Theory* (2006), second edi edn.

16. Januzzi, J. L. Troponin testing after cardiac surgery. *HSR proceedings intensive care & cardiovascular anesthesia* **1**, 22–32 (2009).

Acknowledgements

We thank Dr. Jun-Yi Leu for yeast experimental part and Dr. Chuang-Rung Chang provided mitoGFP strain. This work was supported by the Ministry of Science and Technology (Taiwan).

Additional information

Sources codes are in Supplemental Materials